Engineering 7 (2021) 1149–1156

Contents lists available at ScienceDirect

Engineering

journal homepage: www.elsevier.com/locate/eng

Research
Microecology—Article

Engineered Biomimetic Platelet Membrane-Coated Nanoparticles Block *Staphylococcus aureus* Cytotoxicity and Protect Against Lethal Systemic Infection

Jwa-Kyung Kim [a,b,c,*], Satoshi Uchiyama [c], Hua Gong [d], Alexandra Stream [c], Liangfang Zhang [d,e], Victor Nizet [c,f,*]

[a] *Division of Nephrology, Department of Internal Medicine & Kidney Research Institute, Hallym University Sacred Heart Hospital, Anyang 14068, Republic of Korea*
[b] *Department of Clinical Immunology, Hallym University Sacred Heart Hospital, Anyang 14068, Republic of Korea*
[c] *Division of Host–Microbe Systems and Therapeutics, Department of Pediatrics, University of California San Diego, La Jolla, CA 92093, USA*
[d] *Department of NanoEngineering, University of California San Diego, La Jolla, CA 92093, USA*
[e] *Moores Cancer Center, University of California San Diego Health, La Jolla, CA 92037, USA*
[f] *Skaggs School of Pharmacy and Pharmaceutical Sciences, University of California San Diego, La Jolla, CA 92093, USA*

ARTICLE INFO

Article history:
Received 26 June 2020
Revised 5 September 2020
Accepted 7 September 2020
Available online 1 December 2020

Keywords:
Nanoparticle
Nanosponge
Platelet
Staphylococcus aureus
Bacterial toxins
Sepsis

ABSTRACT

Staphylococcus aureus (*S. aureus*) is a leading human pathogen capable of producing severe invasive infections such as bacteremia, sepsis, and endocarditis with high morbidity and mortality, exacerbated by the increasingly widespread antibiotic resistance exemplified by methicillin-resistant strains (MRSA). *S. aureus* pathogenesis is fueled by the secretion of toxins—such as the membrane-damaging pore-forming α-toxin, which have diverse cellular targets including the epithelium, endothelium, leukocytes, and platelets. Here, we examine the use of human platelet membrane-coated nanoparticles (PNPs) as a biomimetic decoy strategy to neutralize *S. aureus* toxins and preserve host cell defense functions. The PNPs blocked platelet damage induced by *S. aureus* secreted toxins, thereby supporting platelet activation and bactericidal activity. Likewise, the PNPs blocked macrophage damage induced by *S. aureus* secreted toxins, thus supporting macrophage oxidative burst, nitric oxide production, and bactericidal activity, and diminishing MRSA-induced neutrophil extracellular trap release. In a mouse model of MRSA systemic infection, PNP administration reduced bacterial counts in the blood and protected against mortality. Taken together, the results from the present work provide a proof of principle of the therapeutic benefit of PNPs in toxin neutralization, cytoprotection, and increased host resistance to invasive *S. aureus* infection.

1. Introduction

Platelets are abundant, small anucleate cell fragments in the blood circulation. The classical function of platelets involves the regulation of blood clotting and vascular integrity. However, emerging evidence has revealed a role of platelets as sentinel effector cells during infectious diseases [1–3]. Innate immune responses to invading pathogens are significantly influenced by crosstalk with platelets, as the latter can sense and react to danger signals and guide leukocytes to sites of injury, inflammation, or pathogen invasion [4–7].

Platelets have multiple identified roles relevant to host defense [1,2,8,9]. They can directly kill microbes by the release of antimicrobial peptides including defensins [10], cathelicidins [11], thrombocidins [12], and kinocidins [13]. Platelets can also aggregate to entrap microbes and restrict pathogen spread [14]. Through various different mechanisms, platelets regulate the release of a variety of intracellular mediators that are stored in granules [3]. These molecules can induce inflammation and influence the recruitment and activity of effector cells of the immune system directly or indirectly [15]. The mechanisms governing platelet–leukocyte and platelet–microbe interactions are complex, reflecting the diversity of platelet receptors such as complement

* Corresponding authors.
E-mail addresses: kjk816@hallym.or.kr (J.-K. Kim), vnizet@health.ucsd.edu (V. Nizet).

https://doi.org/10.1016/j.eng.2020.09.013

receptors [16], Fc-γ receptor IIa [17], Toll-like receptors (TLRs) [18], glycoprotein (GP)IIb–IIIa [19], and GPIb [20]. In sum, platelets are more than just clotting agents; they are critical players in the fine equilibrium of host immune and inflammatory responses.

Staphylococcus aureus (*S. aureus*), including methicillin-resistant strains (MRSA), is a leading opportunistic Gram-positive bacterial pathogen that produces a wide array of diseases, including invasive bloodstream infections, sepsis, and endocarditis [21,22]. Deep-seated *S. aureus* infections are usually accompanied by clear immune dysregulation, provoked in part by an array of secreted toxin virulence factors, including α-toxin. *S. aureus* toxins can engage cognate surface receptors on host cells and compromise their integrity and function by the formation of membrane pores, disruption of signal transduction pathways, or activation of enzymes that degrade host molecules [23,24]. As secreted toxins play important roles in driving *S. aureus* disease pathogenesis, methods to remove or counteract toxins have become a potential therapeutic target to improve patient outcomes. In this regard, targeted antibody or nanomedicine approaches for toxin neutralization have gained attention [25–27]. One such approach for biodetoxification involves natural cell-membrane-coated nanoparticles that function through biomimicry [28,29]. Their unique structure allows these nanoparticles to function as decoys to absorb bacterial membrane toxin factors nonspecifically like a sponge, thereby neutralizing the factors cytolytic activity regardless of their precise molecular architecture [30]. For example, red blood cell (RBC) membrane-coated "nanosponges" developed by coating polymeric nanoparticles with natural erythrocyte membranes protected mice against lethal intoxication with purified α-toxin protein [31] and reduced lesion size in murine models of MRSA or group A *Streptococcus* skin infection [32,33]. In a mouse model of *Escherichia coli* sepsis, macrophage membrane-coated nanosponges bound bacterial lipopolysaccharide (LPS) and sequestered proinflammatory cytokines, thereby reducing bacterial spread and conferring protection against mortality in the treated mice [34].

Platelets have been shown to contribute to host resistance against invasive *S. aureus* infection. Antibody-mediated platelet depletion in mice impaired *S. aureus* clearance, as evidenced by higher bacterial burden in kidneys, more exaggerated cytokine responses, and decreased survival compared with control mice [35]. Another study indicated that platelets enhanced the uptake and intracellular killing of *S. aureus* by peritoneal macrophages, perhaps through a mechanism dependent on platelet granule-associated β1-defensin [8]. Platelets are an important target of *S. aureus* α-toxin, as they express a disintegrin and metalloproteinase domain-containing protein 10 (ADAM10), the identified α-toxin receptor, on their surface membrane [36]. In mice, α-toxin-mediated platelet damage and aggregation contribute to liver injury in *S. aureus* sepsis [37].

As platelets are both important in the defense against *S. aureus* and the target of the pathogen's membrane toxins, we hypothesized that biodegradable polymeric nanoparticle cores coated with biomimetic human platelet membranes, or platelet membrane-coated nanoparticles (PNPs), could be used to fortify platelet-mediated defense against the pathogen. The present work provides a proof of principle of the therapeutic benefit of PNPs in toxin neutralization, cytoprotection, and increased host resistance to invasive *S. aureus* infection.

2. Materials and methods

2.1. Platelet membrane derivation

Blood-bank-approved human O-negative (universal donor) platelet-rich plasma (PRP) stored in standard acid-citrate-dextrose (ACD) was obtained within 24–48 h of its expiration for clinical use from the San Diego Blood Bank; this PRP serves as a source of fully functional platelet membranes, based on our prior investigations [38]. Phosphate-buffered saline (PBS) solution with 50 $mmol \cdot L^{-1}$ ethylenediaminetetraacetic acid (EDTA; Thermo Fisher Scientific, USA) and 300 μL protease inhibitor (PI; Thermo Fisher Scientific, USA) was added to the PRP preparation to restrict platelet activation. Platelets were centrifuged at 4000 revolutions per minute (rpm) for 15 min at room temperature; the supernatant was then discarded, and the pelleted platelets were resuspended in PBS + 1 $mmol \cdot L^{-1}$ EDTA and PI tablets.

2.2. Platelet nanosponge preparation

Aliquots (1.2 mL) of platelet preparation (~3×10^9 cells) were used to coat the 1 mg of poly(lactic-*co*-glycolic acid) (PLGA) core. Platelet membrane suspensions were derived through three cycles of freeze-thawing: The aliquots were first frozen at −80 °C, then thawed to room temperature, and then centrifuged at 8000 relative centrifugal force (rcf) for 7 min for pelleting. Finally, they were resuspended in water and quantified via the Pierce BCA protein assay kit (Thermo Fisher Scientific, USA). PNPs were derived in two stages: First, approximately 80 nm polymeric cores were prepared by nanoprecipitation using 0.67 $dL \cdot g^{-1}$ carboxyl-terminated 50:50 PLGA (LACTEL absorbable polymers) dissolved in acetone at 10 $mg \cdot mL^{-1}$; 1 mL of the dissolved PLGA was quickly added to 3 mL of water, and the open mixture was stirred for 12 h to evaporate the acetone to a final nanoparticle concentration of 2.5 $mg \cdot mL^{-1}$. Second, the platelet membrane preparations were combined with the nanoparticle cores at a 1:1 ratio (membrane protein to polymer weight). Platelet membrane vesicles were dispersed and fused with the PLGA particles via sonication using a frequency of 42 kHz and a power of 100 W for 5 min to achieve membrane coating.

2.3. Analysis of PNP size distribution and coating

A 1:1 membrane protein-to-polymer weight ratio yielded particles slightly larger than the PLGA core with a surface zeta potential approaching that of the platelet membrane-derived vesicles, confirming successful membrane coating. Indeed, the coating enhanced the colloidal stability of the PLGA cores, which are prone to aggregate under physiological salt concentrations. The PNPs in this study were analyzed by dynamic light scattering (Zetasizer Nano ZS ZEN 3600; Malvern Panalytical Ltd., UK) in triplicate for size and consistency. For transmission electron microscopy (TEM), the PNPs were laid on a 400 mesh carbon-coated copper grid (Electron Microscopy Sciences, USA) stained with 1% uranyl acetate (EM Sciences, USA), and studied under a Zeiss Libra 120 PLUS energy filter transmission electron microscope (EF-TEM, Germany).

2.4. Bacterial strains and α-toxin

MRSA strain USA300/TCH1516 and its isogenic human leukocyte antigen (HLA) mutant (Sun BioRxiv, USA) were used in this study. Strains were propagated in Todd–Hewitt broth (THB; Thermo Fisher Scientific, USA) at 37 °C to mid-logarithmic phase (optical density 600 nm (OD_{600}) = 0.4), pelleted by centrifugation at 4000 rpm for 10 min, washed once, and then resuspended to the desired dilution in PBS. Bacterial inocula-confirmed dilution plating was performed for colony-forming units (CFU). Recombinant α-toxin was purchased from Sigma-Aldrich (#H9395; USA).

2.5. Platelet isolation

Human venous blood was collected by simple phlebotomy from healthy human donors under informed consent and anticoagulated with ACD (1:6 v/v; Sigma-Aldrich, USA). PRP was prepared from blood centrifuged at 1000 rpm for 10 min with no brake, using only the upper two thirds of the PRP fractions to avoid leukocyte contamination. Platelets were isolated from PRP by centrifugation for 10 min at 1500 rpm, and then resuspended in serum-free Roswell Park Memorial Institute (RPMI) 1640 media (Thermo Fisher Scientific, USA) at room temperature.

2.6. Platelet cytotoxicity assay

Human platelets (1×10^7 per well) pretreated with PNPs ($1\ mg{\cdot}mL^{-1}$) or vehicle control were placed at room temperature for 30 min, and then exposed to 3 μL supernatant of MRSA culture for 1 h. Samples were centrifuged for 5 min at 500*g* ($g = 9.8\ m{\cdot}s^{-2}$), and lactate dehydrogenase (LDH) released from platelets into the media was determined using the Promega assay.

2.7. Platelet bactericidal assay

To evaluate the bacterial killing by isolated platelets, isolated platelets were first pretreated with $1.0\ mg{\cdot}mL^{-1}$ of PNPs or vehicle control for 30 min at room temperature, and then infected for 1 h with 10 μL of MRSA at multiplicity of infection (MOI) = 0.1 bacteria per platelet. For CFU enumeration and to calculate the percent of MRSA killing in comparison with the original inoculum, the dilution plates were sonicated by Sonic Dismembrator 550 (Thermo Fisher Scientific, USA) for 3 s.

2.8. Platelet activation assay

MRSA supernatants were collected by the centrifugation (4000 rpm for 15 min) of bacterial culture grown overnight in THB media at 37 °C. Next, 1×10^7 platelets were treated with 1.25–2.5 μL MRSA supernatant premixed witsupernatant of MRSA cultureh PNPs or vehicle control. After incubation at 37 °C, the samples were stained with phycoerythrin (PE) anti-human CD62p (P-selectin) antibody (Biolegend, USA) for 20 min at room temperature, and then diluted in 1 mL PBS. The expression of P-selectin was measured by FACSCalibur flow cytometry (BD Biosciences, USA) and analyzed using FlowJo v10.2 software (Becton, Dickinson and Company, USA). Human platelets and PNPs were separated by size gating; the human platelet population was then analyzed for mean fluorescence of PE.

2.9. Macrophage preparation and cell viability assays

Human myeloid leukemia monocytes (THP-1) (American Type Culture Collection (ATCC), USA) were cultured in RPMI + 10% fetal bovine serum (FBS). The THP-1 were differentiated into macrophages with 25 $nmol{\cdot}L^{-1}$ phorbol 12-myristate 13-acetate (PMA; Sigma-Aldrich, USA) for 48 h followed by a 24 h cooldown period in RPMI + 10% FBS. For THP-1 cytotoxicity, 5×10^5 THP-1 were plated in each well and pretreated with $1\ mg{\cdot}mL^{-1}$ of PNPs or vehicle control for 30 min at room temperature, and then exposed to a range of MRSA supernatant doses (1.25–10.00 μL) for 1 h at 37 °C. The viability of THP-1 and THP-1 differentiated macrophages was measured using the 3-(4,5-dimethylthiazol-2-yl)-2,5-diphenylte-trazolium bromide (MTT) cell proliferation assay kit (ab211091; Abcam plc., USA), which quantifies adenosine triphosphate (ATP) conversion of MTT to formazan as read by absorbance at 590 nm.

2.10. Macrophage bactericidal assays

For THP-1 differentiated macrophage bactericidal assays, differentiated macrophages were treated with $1\ mg{\cdot}mL^{-1}$ PNPs or vehicle control for 30 min, and then infected with MRSA at MOI = 1.0 bacteria per cell. Cells were lysed using Triton X-100 (0.025%; Sigma-Aldrich, USA), and serially diluted for CFU enumeration and the calculation of percent MRSA killing in comparison with the original inoculum.

2.11. Macrophage oxidative burst and nitric oxide production assays

For oxidative burst assays, THP-1 differentiated macrophages were loaded with 25 $\mu mol{\cdot}L^{-1}$ 2,7-dichlorofluorescein diacetate (DCFH-DA; Thermo Fisher Scientific, USA) in Hank's balanced salt solution (HBSS; Mediatech, USA) lacking Ca^{2+} and Mg^{2+}, and rotated at room temperature for 30 min. Macrophages were then infected with MRSA (MOI = 1.0 bacteria per cell) with or without PNPs, and incubated at 37 °C. Every 15–30 min, the fluorescence intensity at 485 nm excitation/520 nm emission was compared by SpectraMax M3 (Molecular Devices, USA). For quantifying the nitrite production in THP-1 differentiated macrophages under the same exposure conditions, Greiss reagent (Promega, USA) was used according to the manufacturer's protocol.

2.12. Human neutrophil extracellular trap staining and quantification

Neutrophils were isolated from blood collected from healthy adult human donors who had given informed consent, using PolymorphPrep (Progen Biotechnik GmbH, Germany) according to the manufacturer's instructions. Next, 5×10^5 neutrophils were placed in the wells of a 24-well plate, stimulated with vehicle control, 25 $nmol{\cdot}L^{-1}$ PMA, MRSA alone, or MRSA premixed with PNPs for 20 min (MOI = 10 bacteria per neutrophil), and incubated for 3 h at 37 °C. For visualization, cells fixed in 4% paraformaldehyde were stained with an antibody against myeloperoxidase (MPO) (1:300; Calbiochem, USA) in PBS + 2% bovine serum albumin (BSA; Sigma-Aldrich, USA) for 1 h, then placed in Alexa Fluor 488 goat anti-rabbit (1:500; Life Technologies, USA) for 45 min, and finally counterstained with 1 $\mu mol{\cdot}L^{-1}$ Hoechst-3342-trihydrochloride diluted in 2% PBS–BSA for 10 min before imaging was carried out on a fluorescence microscope. In parallel, neutrophil extracellular traps (NETs) were quantified using the Quant-iTTM PicoGreen dsDNA assay kit (Invitrogen, USA) on wells in which micrococcal nuclease solution was added to release the DNA of the NETs into the supernatant; 500 $mmol{\cdot}L^{-1}$ EDTA was added to the solution to stop the micrococcal nuclease reaction. PicoGreen solution was prepared according to the manufacturer's instructions and incubated for 5 min; fluorescence signals were then measured with filter settings of 480 nm excitation/520 nm emission.

2.13. Cytokine quantification assays

Cytokines interleukin (IL)-8 and IL-1β were quantified from infected THP-1 differentiated macrophage cell supernatants (4, 8, and 24 h post-infection) using enzyme-linked immunosorbent assay (ELISA) kits (R&D systems, USA) according to the manufacturer's protocol. Experiments were conducted in triplicate or quadruplicate.

2.14. In vivo *murine* S. aureus *infection experiments*

For survival studies, MRSA cultures were grown in THB to mid-log phase and washed once in PBS. Next, 3×10^8 CFU was intraperitoneally (i.p.) injected in outbred, 10–12 week-old, CD1 mice (Charles River, USA). For the PNP treatment group, 100 μL

of a 5 mg·mL^{-1} of PNPs was injected intravenously (i.v.) twice, immediately after MRSA infection and 3 h after the first injection. Survival was monitored daily for 6 d. In a separate challenge experiment using the same MRSA challenge dose and PNP treatment protocol, mice were sacrificed at 6 h for the determination of bacterial CFU units and the quantification of tumor necrosis factor (TNF) and IL-6 in serum and spleen.

2.15. Statistical analyses

All studies were conducted in duplicate or triplicate and repeated independently at least twice. All data are graphed as means with standard error of the mean (SEM) or standard deviation (SD). Statistical evaluation was done by one-way analysis of variance (ANOVA) or unpaired two-tailed Student's *t*-test (Graph Pad Prism 5.03) (*: $P < 0.05$; **: $P < 0.01$; ***: $P < 0.001$).

2.16. Ethical approval

Animal studies were conducted in accordance with protocols approved by the UC San Diego Institutional Animal Care and Use Committee (IACUC; protocol S00227M); all efforts were made to reduce animal numbers and minimize suffering. Blood for platelet isolation was obtained via venipuncture from healthy volunteers under written informed consent approved by the UC San Diego Human Research Protection Program.

3. Results

3.1. Preparation and analysis of PNPs

In this study, our goal was to construct PNPs composed of a PLGA polymer core wrapped in natural platelet bilayer membranes. The platelet membrane shell provides a faithful mimicry of the parent platelet surface and can thus absorb the toxin virulence factors of the MRSA of diverse molecular structures, with the aim of reducing platelet toxicity and preserving platelet defense function against MRSA infection (Fig. 1(a)). Cell membranes from recently expired (< 24–48 h) blood-bank-approved platelet concentrates from hypotonic lysis, mechanical disruption, and differential centrifugation have been found to retain membrane composition and attendant functions [38]. EDTA was used as the anticoagulant to chelate divalent cations including calcium and avoid activating coagulation processes while stabilizing the platelets [38]. Furthermore, a PI was added to block platelet aggregation [38]. A sonication procedure yielded membrane vesicles for fusion onto PLGA cores to create the final PNPs. The inner polymeric core stabilizes the outer membrane from collapsing and fusing with other membranes, optimizing *in vitro* and *in vivo* stability. After membrane coating, the PNP diameter increased from (88.4 ± 5.6) to (120.0 ± 4.8) nm as assessed by dynamic light scattering, reflecting the encapsulation of the polymeric cores with a cell membrane bilayer (Figs. 1(b) and (c)). TEM clearly showed PLGA polymer cores uniformly coated by a unilamellar membrane, indicating successful PNP formation (Fig. 1(d)).

3.2. PNPs prevent human platelet damage and dysfunction induced by MRSA supernatants

Bacterial toxins including *S. aureus* α-toxin can damage and inhibit the functions of host cells [35,39]. We first investigated whether PNPs could protect intact human platelets against the cytotoxic effect of MRSA supernatants. When human platelets were incubated with MRSA supernatant for 1 h, a significant LDH release reflecting platelet damage was seen; however, this was significantly diminished in the presence of PNPs: The LDH release was 0.52 ± 0.13 (optical density (OD) value) in MRSA supernatant alone, in comparison with 0.27 ± 0.08 (OD value) with PNP treatment ($P = 0.002$) (Fig. 2(a)). The activation of platelets associated with the release of antimicrobial peptide-rich α granules [2] can be

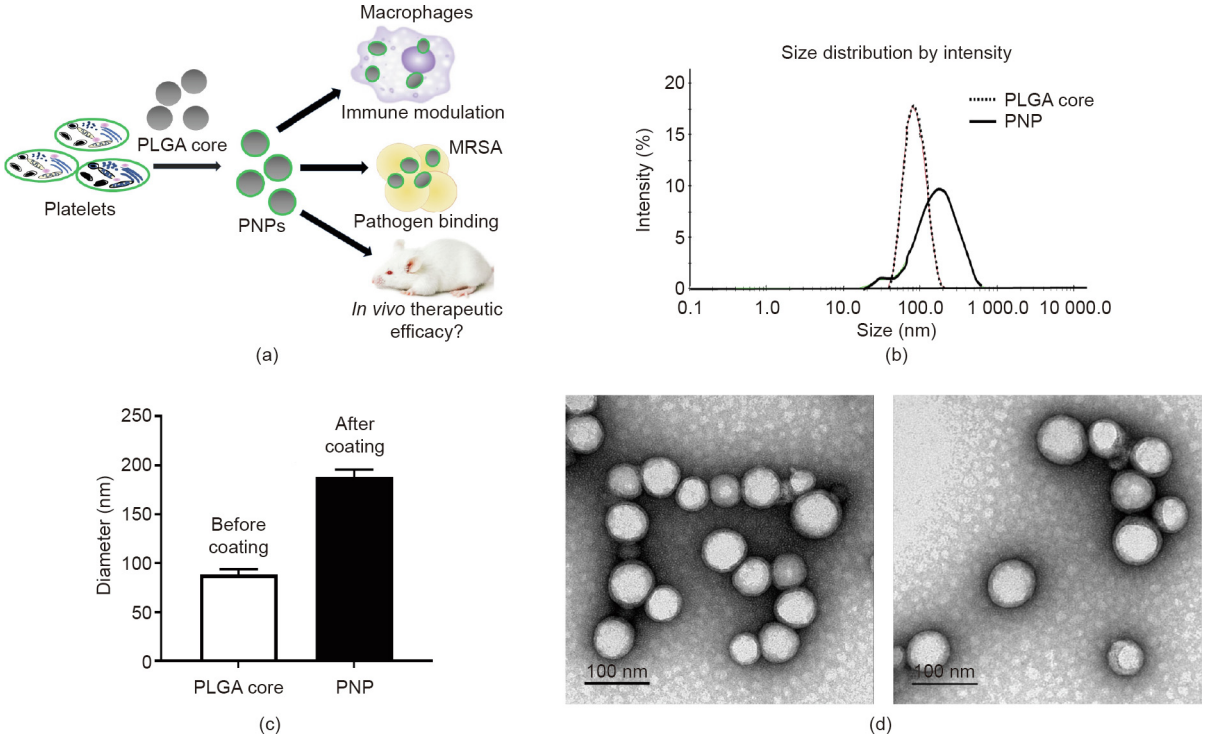

Fig. 1. Formulation and analysis of PNPs. (a) Model showing our rationale of applying PNPs to modulate immune cells, pathogen binding, and control *in vivo* therapeutic efficacy. (b, c) Dynamic light scattering to evaluate hydrodynamic size (diameter in nm) of the PLGA polymeric cores before and after platelet membrane coating. (d) TEM images of the derived PNPs using uranyl acetate counterstain.

quantified by the surface expression of P-selectin. Upon exposure of human platelets to MRSA supernatants, we found that co-incubation with PNPs significantly reduced the time to P-selectin expression and significantly increased the intensity of its expression (Figs. 2(b) and (c)), indicating that PNPs could help to preserve this key platelet response function. To examine whether platelet cytoprotection and functional activation improved innate immune activity, MRSA killing by platelets was assessed in the presence or absence of PNPs. A significant enhancement of platelet MRSA killing was seen upon PNP treatment (Figs. 2(d) and (e)), suggesting that the protective effect of PNPs on MRSA-induced platelet injury might improve the host defense function.

3.3. PNPs prevent human macrophage damage and dysfunction induced by MRSA supernatants

The effect of MRSA supernatants on the viability of THP-1 was examined with or without preincubation of the MRSA supernatant with PNPs for 30 min beforehand. As shown in Fig. 3(a), a nearly 75% reduction in LDH release was observed in the presence of

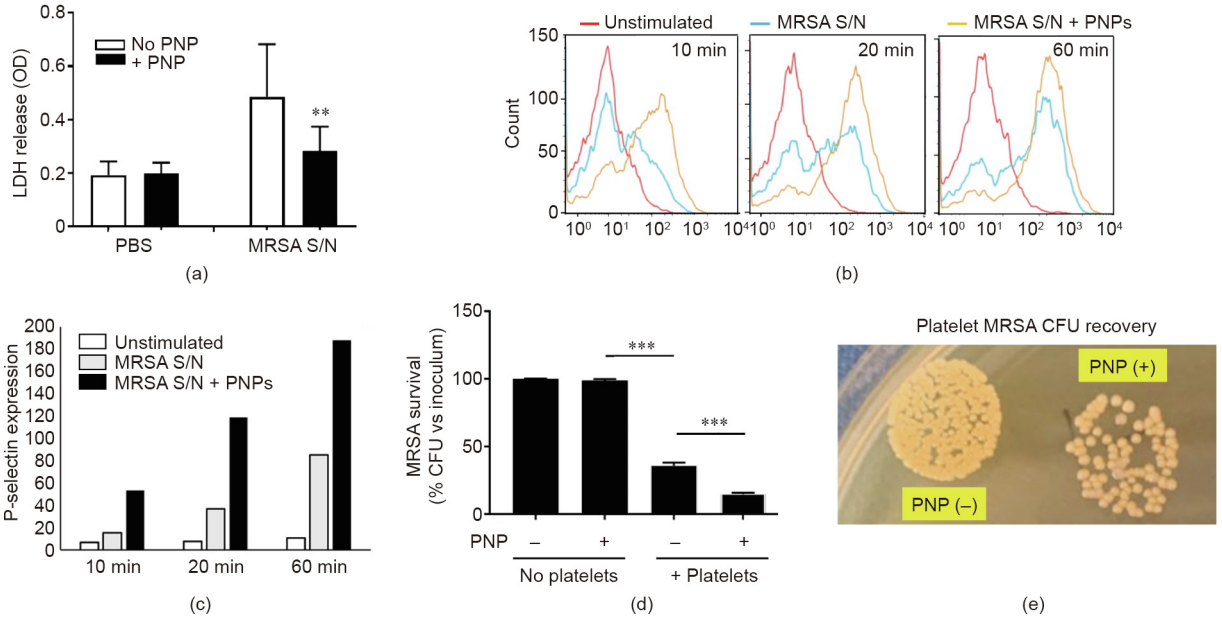

Fig. 2. PNPs prevented human platelet damage and dysfunction induced by MRSA supernatants (S/N). (a) PNP reduced MRSA supernatant-induced platelet cytotoxicity as measured by LDH release with OD value; the cytotoxicity was 0.52 ± 0.13 in MRSA supernatant alone, 0.27 ± 0.08 with PNP treatment (P = 0.002). (b, c) P-selectin expression on platelets exposed to MRSA supernatant in the presence or absence of PNPs. PNP treatment led to a striking increase of P-selectin expression beginning at the early time point (10 min). (d, e) Increased platelet viability upon PNP treatment is accompanied by improved MRSA killing. **: P < 0.01; ***: P < 0.001.

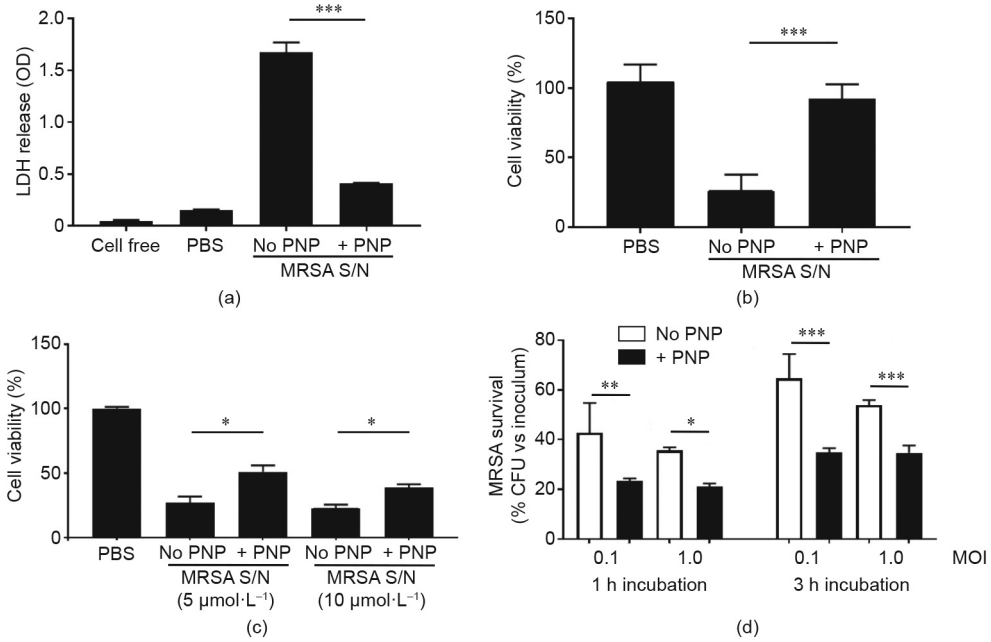

Fig. 3. PNPs prevented macrophage damage and dysfunction induced by MRSA supernatants (S/N). (a) LDH cytotoxicity test and (b) MTT assay indicated that PNP treatment showed about 75% reduction of THP-1 cytotoxicity. (c) PNP also improved the viability of THP-1 differentiated macrophages after MRSA supernatant treatment. (d) Pre-treatment of THP-1 differentiated macrophages with PNP showed higher bactericidal efficiency regardless of bacterial load and incubation time. *: P < 0.05; **: P < 0.01; ***: P < 0.001.

PNPs. Cell viability was further assessed by MTT assay, which showed that the viability of THP-1 after 1 h treatment was markedly increased when the MRSA supernatant was premixed with PNPs, in comparison with the control (Fig. 3(b)). LDH release was also measured in the THP-1 differentiated macrophages, and revealed a significant protective effect of PNPs (Fig. 3(c)). Finally, the THP-1 differentiated macrophages were infected with live MRSA in the presence or absence of PNPs, showing that the nanosponge treatment significantly increased macrophage killing of the pathogen (Fig. 3(d)).

3.4. PNP protection against cytotoxicity preserves macrophage and neutrophil effector responses

We further examined the effect of PNPs on certain key macrophage functions involved in the antibacterial response. The generation of reactive oxygen species (ROS), known as oxidative burst, is a key element of macrophage antibacterial defense, as evidenced by the high rate of *S. aureus* infections in nicotinamide adenine dinucleotide phosphate (NADPH) oxidase deficiency (chronic granulomatous disease) patients with impaired oxidative burst function [40]. PNP treatment increased THP-1 differentiated macrophage ROS production in response to MRSA exposure (Fig. 4(a)). Nitric oxide generation by inducible nitric oxide synthase (iNOS) also contributes to antibacterial defense, as corroborated by more severe *S. aureus* infection in iNOS-deficient mice [41]. PNP treatment likewise boosted THP-1 differentiated macrophage nitric oxide production in response to MRSA exposure (Fig. 4(b)). *S. aureus* infection induces macrophage pyroptosis, a cell death program that is dependent on inflammasome activation and associated with IL-1β release [42]. The generation of IL-1β was modestly reduced at the early time point (Fig. 4(c)); this was coincident with reduced LDH release in cytotoxicity assays (Fig. 3(a)), indicating that pyroptosis is one element of the macrophage response to *S. aureus* challenge, and that the degree of associated cytotoxicity and cytokine release can be partially mitigated by PNP toxin absorption. Platelets express the IL-1β receptor (IL-1R) [43], so sequestration of the IL-1β cytokine by PNP may also contribute to the observed difference. Finally, *S. aureus* toxins [44,45] and activated platelets [46] also elicit neutrophil extracellular traps (NETs), with potential proinflammatory and procoagulant effects that may aggravate sepsis [47] or endocarditis [48]. PNP treatment significantly inhibited MRSA-induced NET formation by human neutrophils *in vitro*, as visualized by immunostaining and measured by PicoGreen quantification of released DNA (Figs. 4(d) and (e)).

3.5. PNPs improve survival in a murine MRSA systemic infection model

Our *in vitro* studies described above show that PNPs blocked MRSA-induced platelet and macrophage cytotoxicity, enhancing the antibacterial effectiveness of both cell types. These findings suggest a potential therapeutic benefit of PNPs against *S. aureus* infection *in vivo*. In prior rodent i.v. injection studies for pharmacokinetic and biodistribution assessment, more than 90% of PNPs were distributed to tissues within 30 min, most prominently in the liver and spleen [38]. Importantly, abnormal blood coagulation has not been seen in prior uses of PNPs in murine models of non-infectious indications, including immune thrombocytopenia [49] and atherosclerosis [50]. We challenged groups of eight mice with 3×10^8 CFU MRSA in 100 μL volume i.p. to induce systemic infection. For the PNP treatment group, we injected 5 mg·mL^{-1} PNPs directly into the bloodstream IV immediately after MRSA infection, and again 3 h after the first injection (Fig. 5(a)). The goal of the two doses was to provide a modest extended therapeutic coverage window, seeking to mitigate pathogen-mediated toxic damage, prevent the propagation of cytokine storm, and prevent early death from sepsis. The survival of mice treated with PNP was significantly improved, with 37.5% of mice surviving for 5 d despite the absence of antibiotic therapy, whereas all mice in the control group died within the first 48 h (Fig. 5(b)). In a separate experiment using the same challenge and treatment conditions, we collected blood at 6 h post-MRSA challenge for the determination of bacterial CFU and serum cytokine levels. The two-dose PNP treatment was associated with a significant (P = 0.036) reduction of MRSA CFU in blood (Figs. 5(c) and (d)), and a slight trend toward reduced

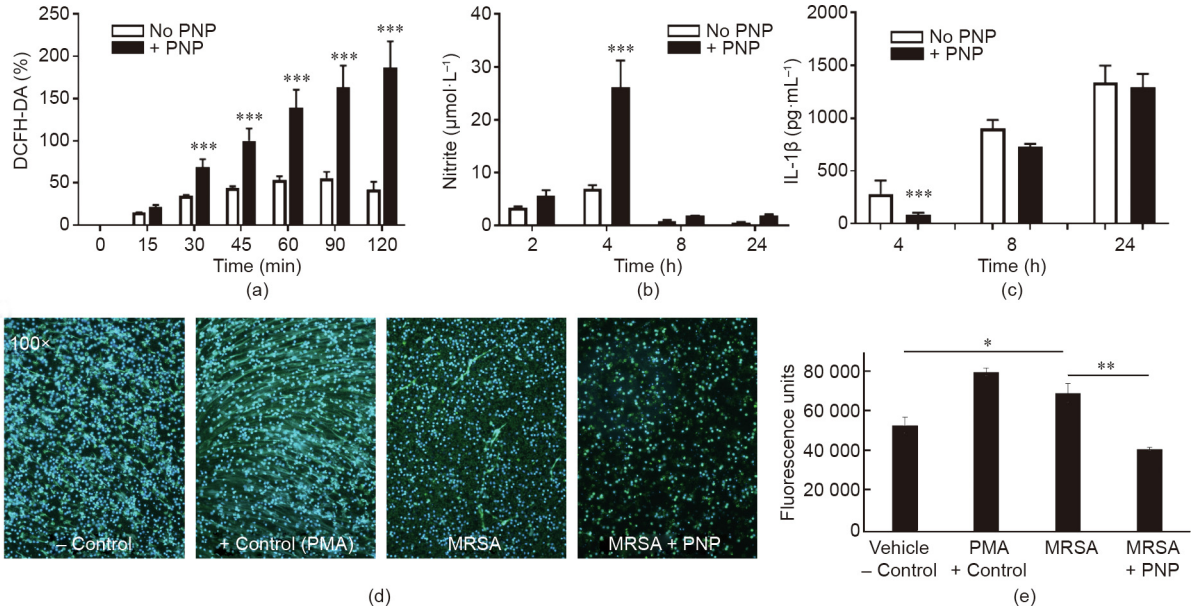

Fig. 4. Effect of PNPs on activation of macrophage and neutrophil bactericidal mechanisms. (a) PNP treatment increases macrophage oxidative burst, as measured by DCFH-DA assay for superoxide production. (b) Increased nitrite production reflecting nitric oxide production was observed in PNP-treated macrophages. (c) Reduced cytokine IL-1β production at the earliest (4 h) time point in PNP-treated macrophages. (d) Immunostaining of human NETs elicited by MRSA in the presence or absence of PNP treatment; PMA serves as a positive control. (e) Quantification of NETs by PicoGreen assay. *: $P < 0.05$; **: $P < 0.01$; ***: $P < 0.001$.

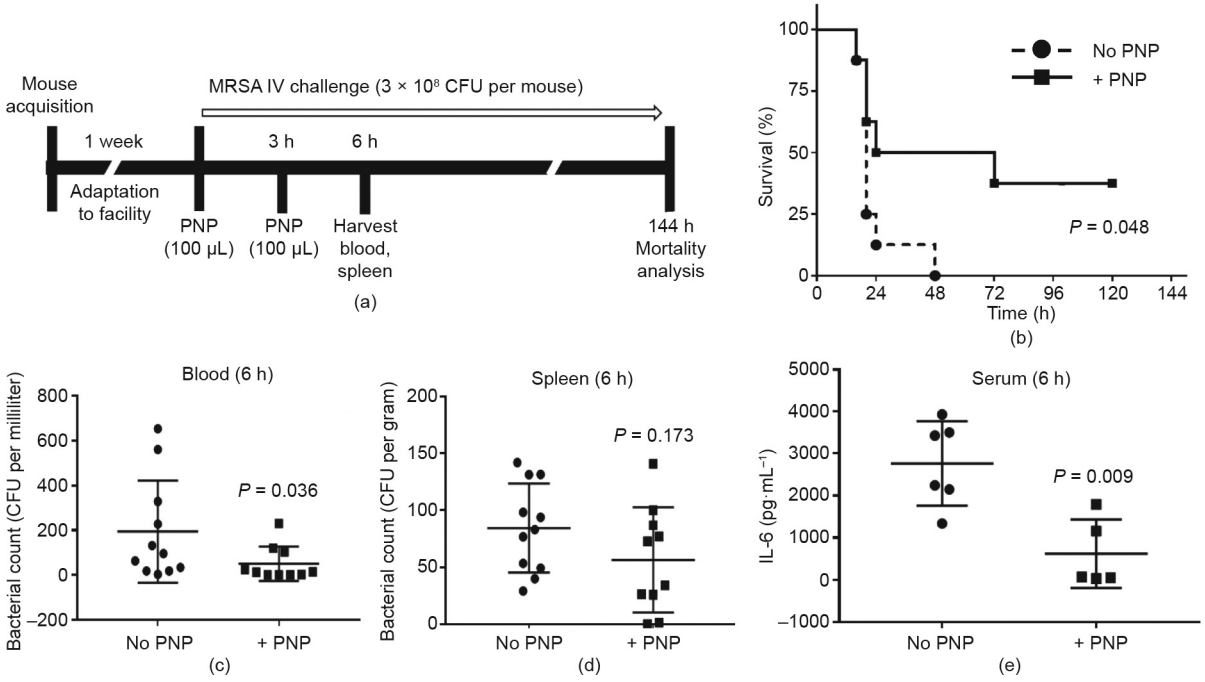

Fig. 5. PNPs improve survival in a murine MRSA systemic infection model. (a) Schematic diagram of the setup of *in vivo* experiments. (b) Survival rates of mice over 144 h following an i.p. injection of MRSA (3×10^8 CFU per mouse). 100 μg PNP at 5 mg·mL^{-1} was injected twice, at 0 and 3 h after bacterial inoculation (n = 8 in each group). Treatment with PNPs provided a significant survival benefit. (c–e) Enhanced bacterial clearance in blood, spleen, and serum during PNP treatment.

counts in the spleen that did not reach statistical significance. Serum IL-6 levels in response to the MRSA challenge were also reduced in the PNP-treated group compared with the control group (Fig. 5(e)).

4. Discussion

In this study, we provided a proof of principle of the therapeutic potential of PNPs in systemic MRSA infection. This benefit is likely multifactorial, and may include: ① reduction of toxin-associated platelet damage, which allows for more rapid and effective deployment of platelet antimicrobial activity; ② protection of phagocytic cells such as macrophages from MRSA cytolytic injury, allowing them to more efficiently deploy ROS and NO and achieve effective bacterial killing; and ③ sequestration of certain bacterial toxins (e.g., pore-forming toxins) in the platelet membrane. Also, since platelets express TLRs (e.g., TLR2) and cytokine receptors (e.g., IL-1R), they could scavenge proinflammatory bacterial cell wall components and cytokines to modulate the hyperinflammation of sepsis. The latter mechanisms would parallel the *in vivo* therapeutic effects of macrophage membrane-coated nanoparticles, which conferred protection against lethality in murine models of LPS endotoxemia and *Escherichia coli* sepsis [34]. While prior work showed that RBC nanosponges protected mice from lethal challenge with whole secreted protein preparations from *S. aureus* supernatants [31], the present work with PNPs is the first report of protection by biomimetic membrane-coated nanoparticles against systemic infection with live *S. aureus*.

A recent study suggests that sepsis contributes as much as 19.7% to human mortality worldwide [51], and there remains no drug specifically approved for the treatment of sepsis [52]. Expanding numbers of antibiotic-resistant bacterial strains such as MRSA further complicate effective sepsis therapeutics [53]. Against this background, the use of PNPs or other cell-membrane-coated nanosponges in sepsis provides a more "universal" approach to the absorption and neutralization of bacterial toxins, in contrast to monoclonal antibodies or other platforms targeting the particular molecular structure of an individual toxin or host inflammatory factor. Other findings that might support an effective therapeutic profile of PNPs include evidence that they reduce macrophage cellular uptake, do not induce human complement activation in autologous plasma, selectively bind to damaged vascular endothelial cells from human and rodents, and likewise bind to platelet-adherent pathogens [31], potentially favoring their accumulation at common sites of endovascular *S. aureus* infection.

In sum, our data suggests that PNPs may protect platelets during systemic MRSA infection by absorbing circulating toxins so that platelets sustain less damage, survive longer, activate more quickly, and have stronger antibacterial effects. PNPs might also protect and support the innate immune function of macrophages or other phagocytic cell types. This biomimetic detoxification strategy merits further exploration as an adjunctive therapy to improve clinicals in patients with MRSA bloodstream, thereby expanding the current approach to clinical management.

5. Limitations of this study

Murine studies of systemic MRSA infection cannot fully recapitulate the tempo and kinetics of human infection, as mice are relatively resistant to the pathogen and very high challenge doses are required to cause organ dissemination and mortality risk. Furthermore, in patients with presumed sepsis, rapid clinical intervention is required—often before microbiological confirmation of the pathogen is established—and patients may have one or more comorbidities that increase the risk of an adverse outcome. Nanosponge therapeutics are thus envisioned as an addition to the standard of care.

Acknowledgements

This work was supported by National Institutes of Health grants HL125352 and U01AI124316 (VN).

Compliance with ethics guidelines

Jwa-Kyung Kim, Satoshi Uchiyama, Hua Gong, Alexandra Stream, Liangfang Zhang, and Victor Nizet declare that they have no conflict of interest or financial conflicts to disclose.

References

[1] Wong CHY, Jenne CN, Petri B, Chrobok NL, Kubes P. Nucleation of platelets with blood-borne pathogens on Kupffer cells precedes other innate immunity and contributes to bacterial clearance. Nat Immunol 2013;14(8):785–92.
[2] Mantovani A, Garlanda C. Platelet–macrophage partnership in innate immunity and inflammation. Nat Immunol 2013;14(8):768–70.
[3] Garraud O, Cognasse F. Are platelets cells? And if yes, are they immune cells? Front Immunol 2015;6:70.
[4] McDonald B, Dunbar M. Platelets and intravascular immunity: guardians of the vascular space during bloodstream infections and sepsis. Front Immunol 2019;10:2400.
[5] Gaertner F, Massberg S. Patrolling the vascular borders: platelets in immunity to infection and cancer. Nat Rev Immunol 2019;19(12):747–60.
[6] Kerris EWJ, Hoptay C, Calderon T, Freishtat RJ. Platelets and platelet extracellular vesicles in hemostasis and sepsis. J Invest Med 2020;68(4):813–20.
[7] Deppermann C, Kubes P. Start a fire, kill the bug: the role of platelets in inflammation and infection. Innate Immun 2018;24(6):335–48.
[8] Ali RA, Wuescher LM, Dona KR, Worth RG. Platelets mediate host defense against *Staphylococcus aureus* through direct bactericidal activity and by enhancing macrophage activities. J Immunol 2017;198(1):344–51.
[9] Ribeiro LS, Migliari Branco L, Franklin BS. Regulation of innate immune responses by platelets. Front Immunol 2019;10:1320.
[10] Valle-Jiménez X, Ramírez-Cosmes A, Aquino-Domínguez AS, Sánchez-Peña F, Bustos-Arriaga J, Romero-Tlalolini MDÁ, et al. Human platelets and megakaryocytes express defensin alpha 1. Platelets 2020;31(3):344–54.
[11] Pircher J, Czermak T, Ehrlich A, Eberle C, Gaitzsch E, Margraf A, et al. Cathelicidins prime platelets to mediate arterial thrombosis and tissue inflammation. Nat Commun 2018;9(1):1523.
[12] Kwakman PHS, Krijgsveld J, de Boer L, Nguyen LT, Boszhard L, Vreede J, et al. Native thrombocidin-1 and unfolded thrombocidin-1 exert antimicrobial activity via distinct structural elements. J Biol Chem 2011;286(50):43506–14.
[13] Trier DA, Gank KD, Kupferwasser D, Yount NY, French WJ, Michelson AD, et al. Platelet antistaphylococcal responses occur through $P2X_1$ and $P2Y_{12}$ receptor-induced activation and kinocidin release. Infect Immun 2008;76(12):5706–13.
[14] Gaertner F, Ahmad Z, Rosenberger G, Fan S, Nicolai L, Busch B, et al. Migrating platelets are mechano-scavengers that collect and bundle bacteria. Cell 2017;171(6):1368–82.
[15] Rossaint J, Margraf A, Zarbock A. Role of platelets in leukocyte recruitment and resolution of inflammation. Front Immunol 2018;9:2712.
[16] Kim H, Conway EM. Platelets and complement cross-talk in early atherogenesis. Front Cardiovasc Med 2019;6:131.
[17] Ilkan Z, Watson S, Watson S, Mahaut-Smith M. $P2X_1$ receptors amplify FcγRIIa-induced Ca^{2+} increases and functional responses in human platelets. Thromb Haemost 2018;118(2):369–80.
[18] Cognasse F, Nguyen KA, Damien P, McNicol A, Pozzetto B, Hamzeh-Cognasse H, et al. The inflammatory role of platelets via their TLRs and Siglec receptors. Front Immunol 2015;6:83.
[19] Berny-Lang MA, Jakubowski JA, Sugidachi A, Barnard MR, Michelson AD, Frelinger AL. $P2Y_{12}$ receptor blockade augments glycoprotein IIb–IIIa antagonist inhibition of platelet activation, aggregation, and procoagulant activity. J Am Heart Assoc 2013;2(3):e000026.
[20] Kroll MH, Harris TS, Moake JL, Handin RI, Schafer AI. Von Willebrand factor binding to platelet GpIb initiates signals for platelet activation. J Clin Invest 1991;88(5):1568–73.
[21] Tong SYC, Davis JS, Eichenberger E, Holland TL, Fowler VG Jr. *Staphylococcus aureus* infections: epidemiology, pathophysiology, clinical manifestations, and management. Clin Microbiol Rev 2015;28(3):603–61.
[22] Turner NA, Sharma-Kuinkel BK, Maskarinec SA, Eichenberger EM, Shah PP, Carugati M, et al. Methicillin-resistant *Staphylococcus aureus*: an overview of basic and clinical research. Nat Rev Microbiol 2019;17:203–18.
[23] Seilie ES, Bubeck Wardenburg J. *Staphylococcus aureus* pore-forming toxins: the interface of pathogen and host complexity. Semin Cell Dev Biol 2017;72:101–16.
[24] Bhakdi S, Tranum-Jensen J. Alpha-toxin of *Staphylococcus aureus*. Microbiol Rev 1991;55(4):733–51.
[25] Fang RH, Luk BT, Hu CMJ, Zhang L. Engineered nanoparticles mimicking cell membranes for toxin neutralization. Adv Drug Deliv Rev 2015;90:69–80.
[26] Cheung GYC, Otto M. The potential use of toxin antibodies as a strategy for controlling acute *Staphylococcus aureus* infections. Expert Opin Ther Targets 2012;16(6):601–12.
[27] Muhammad F, Nguyen TDT, Raza A, Akhtar B, Aryal S. A review on nanoparticle-based technologies for biodetoxification. Drug Chem Toxicol 2017;40(4):489–97.
[28] Fang RH, Kroll AV, Gao W, Zhang L. Cell membrane coating nanotechnology. Adv Mater 2018;30(23):e1706759.
[29] Henry BD, Neill DR, Becker KA, Gore S, Bricio-Moreno L, Ziobro R, et al. Engineered liposomes sequester bacterial exotoxins and protect from severe invasive infections in mice. Nat Biotechnol 2015;33(1):81–8.
[30] Hu CM, Fang RH, Copp J, Luk BT, Zhang L. A biomimetic nanosponge that absorbs pore-forming toxins. Nature Nanotechnol 2013;8(5):336–40.
[31] Chen Y, Zhang Y, Chen M, Zhuang J, Fang RH, Gao W, et al. Biomimetic nanosponges suppress *in vivo* lethality induced by the whole secreted proteins of pathogenic bacteria. Small 2019;15(6):1804994.
[32] Escajadillo T, Olson J, Luk BT, Zhang L, Nizet V. A red blood cell membrane-camouflaged nanoparticle counteracts streptolysin O-mediated virulence phenotypes of invasive group A *Streptococcus*. Front Pharmacol 2017;8:477.
[33] Wang F, Gao W, Thamphiwatana S, Luk BT, Angsantikul P, Zhang Q, et al. Hydrogel retaining toxin-absorbing nanosponges for local treatment of methicillin-resistant *Staphylococcus aureus* infection. Adv Mater 2015;27(22):3437–43.
[34] Thamphiwatana S, Angsantikul P, Escajadillo T, Zhang Q, Olson J, Luk BT, et al. Macrophage-like nanoparticles concurrently absorbing endotoxins and proinflammatory cytokines for sepsis management. Proc Natl Acad Sci 2017;114(43):11488–93.
[35] Wuescher LM, Takashima A, Worth RG. A novel conditional platelet depletion mouse model reveals the importance of platelets in protection against *Staphylococcus aureus* bacteremia. J Thromb Haemost 2015;13(2):303–13.
[36] Maurer S, Kopp HG, Salih HR, Kropp KN. Modulation of immune responses by platelet-derived ADAM10. Front Immunol 2020;11:44.
[37] Surewaard BGJ, Thanabalasuriar A, Zeng Z, Tkaczyk C, Cohen TS, Bardoel BW, et al. α-Toxin induces platelet aggregation and liver injury during *Staphylococcus aureus* sepsis. Cell Host Microbe 2018;24(2):271–84.
[38] Hu CM, Fang RH, Wang KC, Luk BT, Thamphiwatana S, Dehaini D, et al. Nanoparticle biointerfacing by platelet membrane cloaking. Nature 2015;526(7571):118–21.
[39] Thammavongsa V, Kim HK, Missiakas D, Schneewind O. Staphylococcal manipulation of host immune responses. Nat Rev Microbiol 2015;13(9):529–43.
[40] Buvelot H, Posfay-Barbe KM, Linder P, Schrenzel J, Krause KH. *Staphylococcus aureus*, phagocyte NADPH oxidase and chronic granulomatous disease. FEMS Microbiol Rev 2017;41(2):139–57.
[41] McInnes IB, Leung B, Wei XQ, Gemmell CC, Liew FY. Septic arthritis following *Staphylococcus aureus* infection in mice lacking inducible nitric oxide synthase. J Immunol 1998;160(1):308–15.
[42] Accarias S, Lugo-Villarino G, Foucras G, Neyrolles O, Boullier S, Tabouret G. Pyroptosis of resident macrophages differentially orchestrates inflammatory responses to *Staphylococcus aureus* in resistant and susceptible mice. Eur J Immunol 2015;45(3):794–806.
[43] Brown GT, Narayanan P, Li W, Silverstein RL, McIntyre TM. Lipopolysaccharide stimulates platelets through an IL-1 autocrine loop. J Immunol 2013;191(10):5196–203.
[44] Pilsczek FH, Salina D, Poon KKH, Fahey C, Yipp BG, Sibley CD, et al. A novel mechanism of rapid nuclear neutrophil extracellular trap formation in response to *Staphylococcus aureus*. J Immunol 2010;185(12):7413–25.
[45] Malachowa N, Kobayashi SD, Freedman B, Dorward DW, DeLeo FR. *Staphylococcus aureus* leukotoxin GH promotes formation of neutrophil extracellular traps. J Immunol 2013;191(12):6022–9.
[46] Carestia A, Kaufman T, Rivadeneyra L, Landoni VI, Pozner RG, Negrotto S, et al. Mediators and molecular pathways involved in the regulation of neutrophil extracellular trap formation mediated by activated platelets. J Leukoc Biol 2016;99(1):153–62.
[47] Denning NL, Aziz M, Gurien SD, Wang P. DAMPs and NETs in sepsis. Front Immunol 2019;10:2536.
[48] Hsu CC, Hsu RB, Ohniwa RL, Chen JW, Yuan CT, Chia JS, et al. Neutrophil extracellular traps enhance *Staphylococcus aureus* vegetation formation through interaction with platelets in infective endocarditis. Thromb Haemost 2019;119:786–96.
[49] Wei X, Gao J, Fang RH, Luk BT, Kroll AV, Dehaini D, et al. Nanoparticles camouflaged in platelet membrane coating as an antibody decoy for the treatment of immune thrombocytopenia. Biomaterials 2016;111:116–23.
[50] Wei X, Ying M, Dehaini D, Su Y, Kroll AV, Zhou J, et al. Nanoparticle functionalization with platelet membrane enables multifactored biological targeting and detection of atherosclerosis. ACS Nano 2018;12(1):109–16.
[51] Rudd KE, Johnson SC, Agesa KM, Shackelford KA, Tsoi D, Kievlan DR, et al. Global, regional, and national sepsis incidence and mortality, 1990–2017: analysis for the Global Burden of Disease Study. Lancet 2020;395(10219):200–11.
[52] Palma P, Rello J. Precision medicine for the treatment of sepsis: recent advances and future prospects. Expert Rev Precis Med Drug Dev 2019;4(4):205–13.
[53] Uppu DSSM, Ghosh C, Haldar J. Surviving sepsis in the era of antibiotic resistance: are there any alternative approaches to antibiotic therapy? Microb Pathog 2015;80:7–13.